ISSN 1392–1320 MATERIALS SCIENCE (MEDŽIAGOTYRA). Vol. 13, No. 2. 2007

Metallographic Examination of Cast Iron Lump Produced in the Bloomery Iron Making Process

Jonas NAVASAITIS[1], Aušra SELSKIENĖ[2*]

[1]*Kaunas University of Technology, Kęstučio 27, LT-44312 Kaunas, Lithuania*
[2]*Institute of Chemistry, A.Goštauto 9, LT-01108 Vilnius, Lithuania*

Received 01 March 2007; accepted 07 May 2007

A small lump composed of separate cast iron trickles has been discovered during the archaeological investigations of an ancient iron production site in Lieporiai vicinity (Šiauliai district, Lithuania) dating from the 4th to the beginning of the 7th c. AD. A number of peculiarities of this interesting finding, emphasizing its distinction from bloomery iron and even from common cast iron, have been revealed. The results of metallographic examination and the analyses of chemical composition of the lump are presented in the paper.
Keywords: bloomery iron making, cast iron, smelting slag, metallography, chemical composition.

1. INTRODUCTION

Iron occurs in ores as an oxide, but, fortunately, it may be reduced from oxides at the temperatures considerably below its melting point. This property makes bloomery (direct) iron-making process possible. Bloomery furnaces, operating at temperatures 1200 °C – 1300 °C, yielded malleable iron or steel in a solid state as a sponge or raw bloom. However, iron smelted in the bloomeries was occasionally obtained as carbon-rich iron droplets, obviously formed in the liquid state. In all probability the reduced iron grains became heavily carburized in a higher level of the furnace shaft and melted easily to cast iron [1]. This metal was extremely brittle and was not suitable for forging procedures.

Separate iron pieces, created in bloomery furnace, were briefly described in the Polish blacksmith–poet Walenty Rożdzieński's poem written in the early 17th century (1612). The author calls them the *grape* (pronounced *gromp*) [2]. During the sixties in the passed century researchers began examination of these small lumps (usually not exceeding some hundred grammes) composed of metallic iron and smelting slag [3, 4]. Among numerous examined specimens from the first millennium A.D. there were several pieces found to be cast iron produced in bloomery ironworks [3, 5 – 7]. But greater interest concerns some larger lumps weighing up to 36.3 kg. There is a piece (ca 3.5 kg) of hypoeutectic cast iron (1.7 % to 4.3 % C) found in the northern Italy among the bloomery waste of the 5th century A.D. [8]. Microstructure of this lump consists of pearlite, ledeburite and cementite. Another lump of 36.3 kg weight from the Roman period was discovered in Dillingen-Pachten in Saarland. The carbon content in its metallic matrix varies from 1.6 % to 4.5 % C, and its highly heterogeneous structure shows prevailing pearlite with lamellar graphite, ledeburite and cementite [9].

Relatively considerable weight of the lumps led some researchers to the idea that these cast iron samples were an intentionally made product. However, famous Czech scientist R. Pleiner is inclined to see in prehistoric and medieval cast iron samples created in bloomeries as an unwanted product, left in the debris [10]. The beginning of the indirect iron-making process took place in the 13th century A.D. caused by the manganese-rich ores suitable for smelting in *Flossofen* blast furnaces aired by water-powered bellows [11].

A small iron lump (208 grammes) (Fig. 1) was also found in the Lieporian ancient settlement in the Šiauliai district (Lithuania) [12]. There archaeological investigations revealed an iron production site of the late Romano-Barbarian and the early Medieval period [12]. The remains of some twenty small bloomery furnaces, smithery and ca 400 kilograms of smelting slag were excavated in the settlement. According to radiocarbon and dendrochronological dating the iron smelting furnaces and the smithy had been working in the period from the 4th to the beginning of the 7th century AD. However, in the run of ages all furnaces were badly destroyed by human activities, including ancient settlements in the site, soil ploughing and the battles of World War II. In addition, many other finds related to iron production have also been found, e.g. small pieces (as large as nuts) of roasted ore, some stone anvils, four wells (there was no natural source of water on the site), small pieces of charcoal, a fragment of tuyere, several crushing stones, etc.

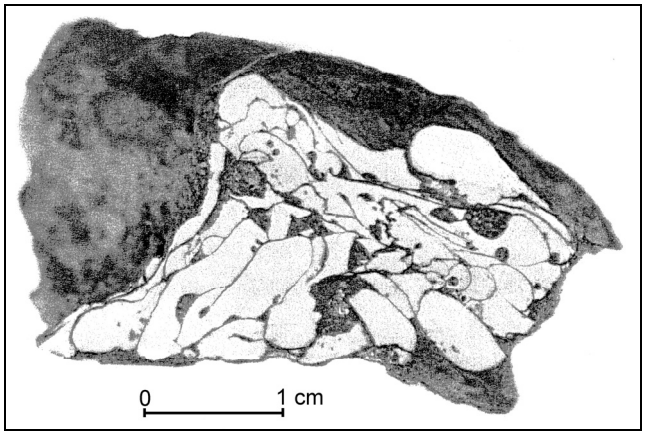

Fig. 1. Cast iron lump from Lieporiai (ŠAM I–A 199:46/2)

*Corresponding author. Tel.: +370-5-2649772; fax: +370-5-2649774.
E-mail adress: *ausra@chi.lt* (A.Selskienė)

At first sight the Lieporian lump bore a resemblance to a piece of tap-slag. Some layer of slag was adhered to it and smooth trickles were solidified on its surface, thus, the lump looked like a piece of tap-slag. Nevertheless, it differed from a bloomery slag in higher density and in strong magnetic permeability. Preliminary examination [13, 14] of the lump has shown it to be created of cast iron trickles forming a compact piece.

The aim of this study is to reveal both the composition of the Lieporian lump and the metallurgical peculiarities of its creation.

2. METHODS OF EXAMINATION

A section composed of several trickles was cut out from the lump for metallographic examination and for analyses of chemical composition both of the metal trickles and of the slag layers (Fig. 2). Slag clots involved in the lump were also examined. The section was mounted in a holder and prepared in the usual manner by grinding and polishing procedures. The macro examination of the lump was performed by conventional methods.

The composition of metal trickles, slag clots and layers was examined by means of the scanning electron microscopes-microanalysers JXA-50A and JEOL JXA 8900 RL at the Vilnius Institute of Chemistry and Johannes Gutenberg University Mainz. In slag analyses the relative error reaches 5 % for Fe, Si and Mn; 10 % for Al, Ca, P, Ti, Mg, K, Na and 30 % for Ba and S. But in a metallic matrix analyses it reaches 1 % for Fe, 10 % for Si and Mn and 30 % for the other elements. The microstructure of the specimens was also examined by optical microscopes LMA – 10 and Neophot 2.

Microhardness of a metallic matrix of the section was tested by means of an apparatus PMT – 3 with the standard square based pyramid and the applied 200 grammes load.

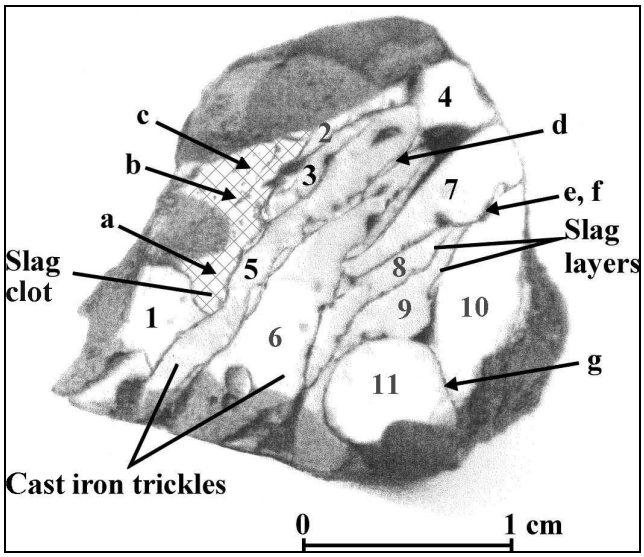

Fig. 2. A macrostructure of a section from the cast iron lump: 1 to 11 – cast iron trickles; a, b, c – examined slag clots; d, e, f, g – examined slag layers in a space between the cast iron trickles

3. RESULTS AND DISCUSSIONS

3.1. Macro and microstructure

Macroanalysis of a polished section of the lump (ŠAM I–A 199:46/2) revealed all the metal trickles separated from each other by a thin layer of slag. Some spaces

Table 1. Microstructure of the cast iron specimen

Trickle No.	Microhardness of matrix (limits) HV_{200} (MPa)	Metallic matrix	Graphite characteristic
1	4580 – 5100	White iron: prevailing columnar cementite in free ferrite, some pearlite	Small graphite nodules
2	1360 – 1530	Grey iron: a dendritic pattern of ferrite	Small graphite flakes, characterized by interdendritic segregation and preferred orientation
3	5130 – 5370	White iron: a dendritic pattern of fine pearlite derived from austenite, and a mixture of massive acicular free cementite with pearlite	Relatively rare fine nodules of graphite evenly distributed along a matrix
4	4490 – 5070	White iron: prevailing columnar cementite in free ferrite	Fine graphite nodules; rare larger graphite nodules
5	4490 – 5070	White iron: prevailing columnar cementite in free ferrite	Small graphite nodules
6	1410 – 2380	Grey iron: a dendritic pattern of ferrite, patches of pearlite	Prevailing interdendritic graphite flakes; rosette grouping of graphite flakes
7	4560 – 5010	White iron: prevailing columnar cementite in free ferrite, some pearlite	Small graphite nodules
8	4560 – 5010	White iron: prevailing columnar cementite in free ferrite, some pearlite	Small graphite nodules
9	1360 – 3800	Columnar cementite in free ferrite, some ferrite dendrites	Small graphite nodules; interdendritic graphite flakes
10	1380 – 2160	Grey iron: ferrite and pearlite	Primary graphite flakes and eutectic graphite
11	1430 – 3890	Prevailing dendritic pattern of ferrite, patches of pearlite, some free cementite in a matrix of ferrite	Prevailing fine graphite flakes characterized by interdendritic segregation and random orientation, some small graphite flakes and nodules

available in the lump are also filled by bloomery slag, thus forming some small slag clots. Smooth open surfaces of the trickles are generally covered by a thin layer of iron oxides. The shape of trickles (Figs. 1 – 2) strongly suggests they have successively solidified one after another and being liquid they possessed rather good fluidity. When running down, liquated slag has spread on the metal trickles covering their surfaces, and in this way, it has formed the slag layers separating the trickles.

The metallographic examination of the section has revealed a great variety of microstructure in this relatively small lump. Separate trickles demonstrate grey, white and mottled iron resulting from variation of both the cooling rate and the chemical composition of respective trickles. Therefore, the variety of a matrix structure and different types of graphite have been found in the sample. The main data of a microstructure of the trickles are given in Table 1.

Grey iron trickles (No. 2, 6, 10, 11 in Fig. 2) are characterized by various types of graphite flakes, distributed in a ferritic or pearlitic matrix. Here one finds randomly distributed primary graphite flakes and eutectic graphite (Fig. 3, a), small graphite flakes characterized by rosette grouping (Fig. 3, b) and fine graphite flakes with interdendritic segregation (Fig. 3, c). Microhardness (HV_{200}) of a metallic matrix of grey iron trickles ranges from 1360 MPa to 2300 MPa.

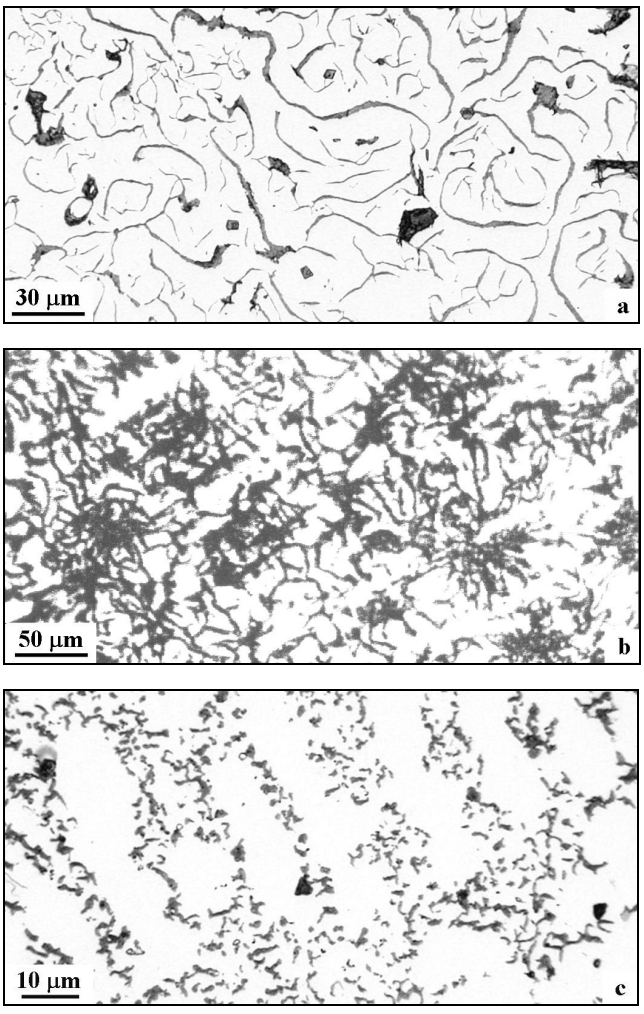

Fig. 3. Graphite flakes in grey iron trickles (not etched): a – primary and eutectic graphite flakes (trickle No.10); b – rosette grouping of graphite flakes (trickle No.6); c – interdendritic segregation of graphite flakes (trickle No.2)

A metallic matrix of white cast iron trickles generally consists of cementite (the majority of columnar shape) in free ferrite. Some areas of the matrix demonstrate a dendritic pattern of fine pearlite and a mixture of coarse free cementite with pearlite (Fig. 4). Microhardness (HV_{200}) of white iron trickles ranges from 4490 MPa to 5370 MPa In addition, small graphite nodules are distributed along all matrix of white iron (Fig. 5). The shape of nodules is similar to that of temper carbon. However, insufficiency of obvious indications on decomposition of cementite in white cast iron matrix does not bear out that the graphite nodules observed would be temper graphite. Hence, the other derivation of considered graphite nodules would not be rejected.

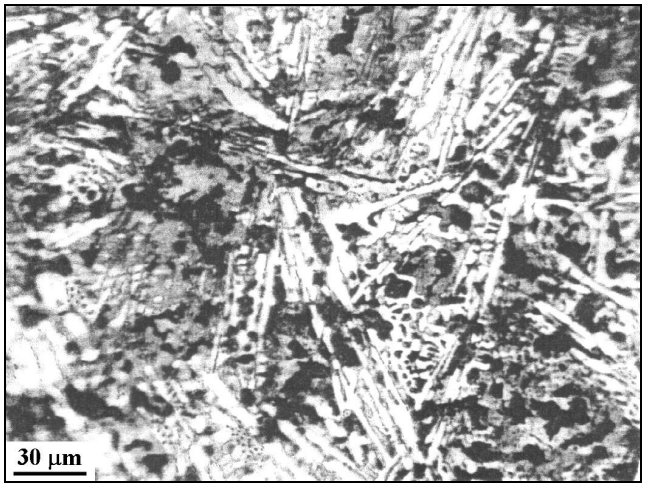

Fig. 4. Microstructure of trickle No.3: hypoeutectic white cast iron, showing a dendritic pattern of pearlite (dark grey), mixture of coarse acicular free cementite (light) with pearlite and small graphite nodules (black) (2 % nital)

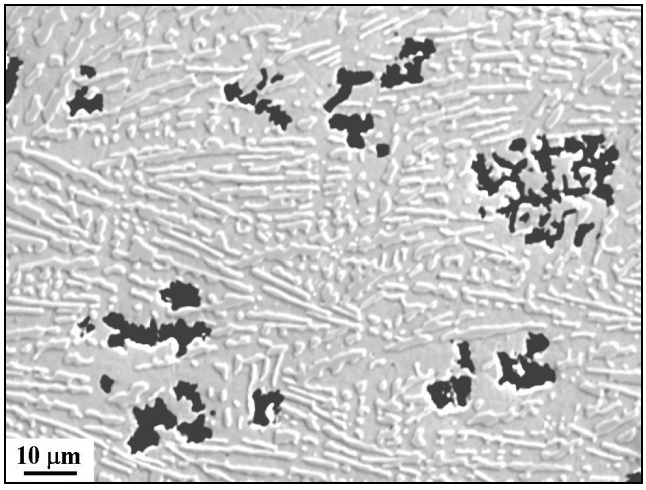

Fig. 5. Graphite nodules in trickle No.3 (not etched): small graphite nodules (black) are distributed along a matrix of white iron (back-scattered electron image)

3.2. Chemical composition

The carbon content of the lump was found to be rather high, but not exceeding the eutectic value. In the examined

sample an average of carbon content reaches ca 3.32 % C showing the lump to be formed of hypo-eutectic cast iron. In addition to carbon, a certain amount of some other elements reduced from the ore has also been detected. Chemical composition of the examined trickles of the lump is given in Table 2.

A glance at Table 2 shows a highly variable concentration of alloying elements present in a metallic matrix of the trickles (unlike to relatively "pure" bloomery iron). At first note a high content of manganese (Mn) and silicon (Si) in particularly that is the other distinct feature of cast iron. The amount of manganese varies from 0.19 % in the 10th trickle to 0.47 % in the 6th trickle, while the silicon content varies from 1.47 % in the 6th trickle to 4.17 % in the 9th trickle. It is important to note a rather high content of manganese (0.23–6.26 %) has been revealed in iron ore residues found in the Lieporian iron smelting site [15].

The free energy changes indicate that reduction of Si and Mn from their oxides is more difficult than that of iron. For example, the temperature required for the reduction of manganese oxides by carbon monoxide is about 1450 °C, while that necessary for silicon oxide would exceed 1550 °C [16]. Therefore, during the normal direct iron smelting in a bloomery furnace Si and Mn usually go into the slag. However, a high amount of manganese and silicon, present in the Lieporian cast iron lump, shows there were the exceptionally reducing conditions in furnace. In addition, silicon can be reduced from oxides at a much lower temperature if metallic iron is participating in the process. In that case the process of silicon reduction already begins at 1050 °C [17]. The formed silicon and iron compounds (Fe_3Si, FeSi, $FeSi_2$) go into solution in the iron resulting in the increase in the silicon content in cast iron.

Manganese content found in all examined trickles is also many times higher than that usually found in bloomery iron. It is most likely that in furnace manganese has been reduced by soot (solid carbon formed during the smelting process from carbon monoxide) as the process of manganese reduction by solid carbon begins at 1100 °C [16]. Under such conditions carbon is present as well forming the iron and manganese carbides and making the reduced iron virtually a cast iron.

Sulphur and phosphorus show great segregation in the lump probably indicating significant heterogeneity of the smelted ores even in relatively small volumes. Phosphorus content in the section, except trickle No. 6, is uniformly low varying from 0 to 0.27 %. But the 6th trickle contains up to 0.72 % P. Sulphur content in the specimen is also low not exceeding 0.08 %, only the 5th trickle demonstrates the amount of sulphur as high as 0.27 %. The analysis has revealed that sulphur distribution in a metallic matrix is coincident with the manganese distribution, thus showing that manganese sulphide has been formed (Fig. 6). Manganese sulphide (MnS) demonstrates very low solubility in iron, therefore it has remained in a smelt in fine suspended particles.

Table 2. Chemical composition of metallic matrix, weight %

Element	Examined trickle					
	5	6		9	10	10
		Dendrite	Interden-dritic area			
	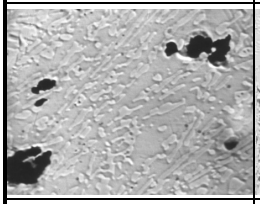	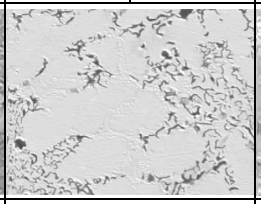		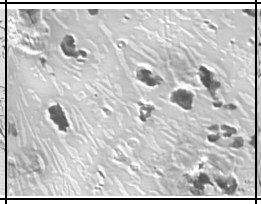	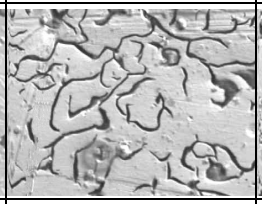	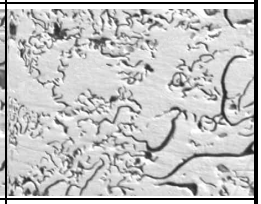
	50 μm	50 μm		50 μm	50 μm	50 μm
Mn	0.26 – 0.40	0.23 – 0.46	0.35 – 0.47	0.29 – 0.32	0.19 – 0.38	0.24
Si	1.57 – 3.07	1.47 – 3.04	1.67 – 2.50	1.79 – 4.17	1.78 – 2.90	1.65
P	0.11 – 0.13	0.03 – 0.72	0.00 – 0.05	0.00 – 0.27	0.03 – 0.15	0.21
S	0.00 – 0.27	0.00 – 0.01	0.04 – 0.08	n.d.	0.00 – 0.02	0.03
Cu	0.02 – 0.08	0.03 – 0.08	0.02 – 0.10	0.04 – 0.09	0.02 – 0.08	0.03
Ni	0.03 – 0.06	0.02 – 0.06	0.03	0.02 – 0.06	0.01 – 0.03	0.04
Co	0.06 – 0.07	0.08 – 0.10	0.07	0.07 – 0.08	0.07 – 0.08	
As	0.00 – 0.03	0.01 – 0.02	0.00 – 0.01	0.00 – 0.01	0.01 – 0.04	0.03
Cr	0.04 – 0.05	0.01	0.03	0.04	0.01	0.01
V	0.00 – 0.06	0.00 – 0.02	0.04	0.00 – 0.01	0.01	
Ti	0.02 – 0.07	0.00 – 0.03	0.03	0.03 – 0.07	0.01 – 0.04	0.05
Zn	n.d.	n.d.	n.d.	0.02	n.d.	
Ca	n.d.	0.01	n.d.	0.01	0.01	n.d.
K	n.d.	n.d.	0.01	0.01	n.d.	n.d.
Fe	94.24 – 94.51	94.46–96.11	90.16	94.59 – 94.75	95.83 – 96.02	95.63

n.d. – not detected.

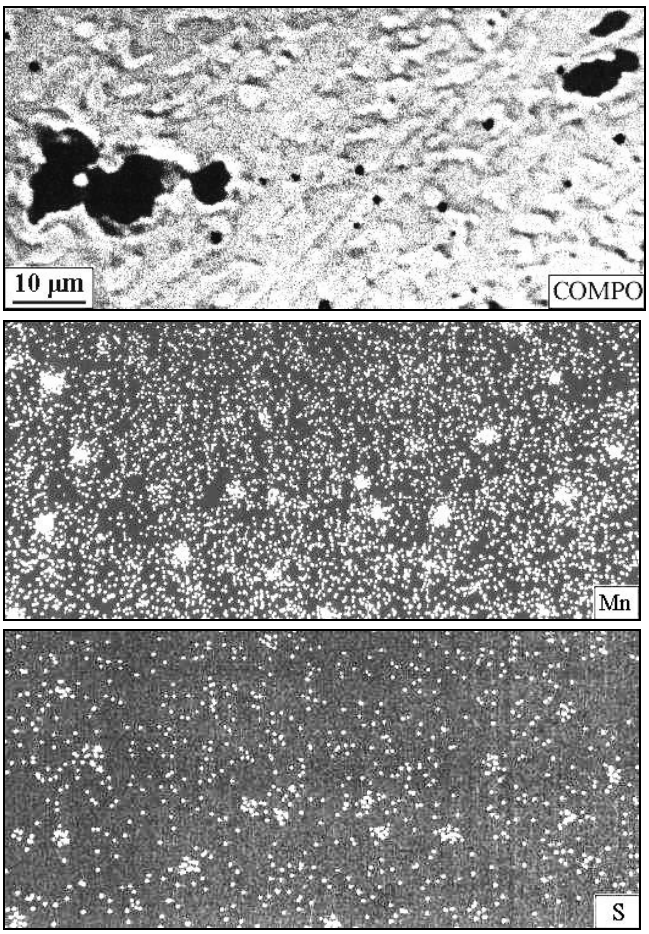

Fig. 6. Manganese sulphide distribution in a metallic matrix of trickle No.5: COMPO – back-scattered electron image (metallic matrix – iron carbides in ferrite, graphite nodules, and fine black spots of MnS distributed along a matrix); Mn and S – distribution of manganese and sulphur, respectively (the density of the light spots is proportional to the relative concentration of the respective element)

Such elements as copper, nickel, cobalt, arsenic can be reduced from their oxides more easily than iron and they enter into solid solution in reduced iron during the smelting process. Nevertheless, the content of Cu, Ni, Co and As in a metallic matrix of the trickles has been found to be uniformly low thus indicating an insignificant amount of these elements in the ores smelted. Many other metals present in the gangue minerals in bog ores are more difficult to reduce. Therefore, only the traces of some of them (Zn, Ca, K) have been found in the lump. Insignificant amounts of Ti, Cr, V are also found.

3.3. Slag clots and layers

In addition to the slag adhered to the lump some clots of slag, involved inside the lump, were observed (Fig. 2). Analyses of slag clots and slag layers entrapped in the lump can yield information on some specific parameters of cast iron formation in a bloomery furnace. The results of analyses are listed in Table 3.

The analyses of the slag clots show a different composition of slag as compared with common bloomery slags produced in a direct iron smelting process. The results of analyses demonstrate a uniformly low iron oxide (FeO) content (from 30.45 % to 34.08 %), but a high silicon oxide (SiO_2) content (from 41.72 % to 46.14 %). In addition, manganese oxide (MnO) is found to be exceptionally high (from 12.16 % to 13.62 %) in the clots. For example, the ordinary Lieporian smelting slag contains ca 65.4 % – 77.1 % FeO, 11.5 % – 26.1 % SiO_2 and only 0.17 % – 0.39 % MnO [15]. No free wüstite (FeO) has been observed, however, rare small rounded droplets of smelted iron were revealed in a monotonous glassy mass of slag. Small quartz grains are also found both in some slag clots (Fig. 7) and the layers (slag layer *f* in Table 3).

The results of the analyses of slag layers, separating the cast iron trickles, indicate them being bloomery slags with prevailing fayalite (Fe_2SiO_4), composed of iron and silicon oxides (Table 3). The ratio of FeO and SiO_2 in fayalite is about 2.4, while in a slag of the layers studied it reaches some lower value ca 2.1. However, these slags contain very high amount of manganese oxide (ca 13.35 % in average), but manganese can partially replace some iron in the slag [18], thus increasing a degree of iron extraction from an ore.

Table 3. Composition of slag clots and layers, weight %

Compounds	Slag clots	Slag layers			
	a, b, c 12 analyses	d 2 analyses	e 2 analyses	f 2 analyses	g 1 analysis
FeO	30.45 – 34.08	51.74 – 58.31	53.90 – 66.43	0.10 – 0.43	44.69
SiO_2	41.72 – 46.14	32.76 – 37.85	14.67 – 26.47	97.81 – 97.88	36.52
MnO	12.16 – 13.62	4.40 – 7.96	12.34 – 14.36	0.07 – 0.15	12.67
P_2O_5	0.15 – 0.23	0.24 – 0.62	0.03 – 0.16	n.d.	0.16
Al_2O_3	4.64 – 4.92	0.04 – 0.08	0.19 – 0.36	n.d.	0.47
CaO	1.66 – 2.56	n.d.	n.d.	≤ 0.01	0.06
MgO	0.34 – 0.42	0.07 – 0.19	n.d.	n.d.	0.63
TiO_2	0.97 – 1.05	0.20 – 0.92	2.47 – 2.72	≤ 0.03	1.81
K_2O	0.24 – 0.39	n.d.	≤ 0.02	≤ 0.02	0.32
Na_2O	0.10 – 0.26	n.d.	≤ 0.01	≤ 0.01	0.22
BaO	n.d.	n.d.	≤ 0.02	≤ 0.04	n.d.
S	0.03 – 0.05	0.04 – 0.14	0.01 – 0.03	≤ 0.01	0.38
Total	97.78 – 99.22	96.77 – 98.78	96.15 – 98.10	98.00 – 98.54	97.93

n.d. – not detected.

A thin film (20 μm – 50 μm) of iron oxide covering the surface of cast iron trickles and separating them from slag clots and layers (Fig. 8) suggests that for some moments cast iron trickles had been in an oxidizing environment and had solidified earlier before slag layers covered the trickles.

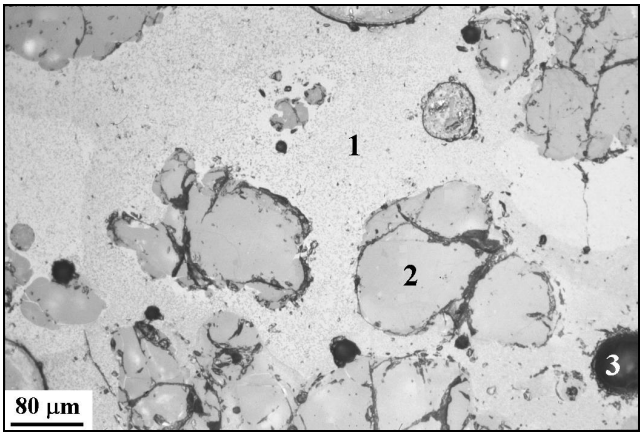

Fig. 7. Microstructure of slag clot: 1 – glassy mass; 2 – quartz grains; 3 – holes

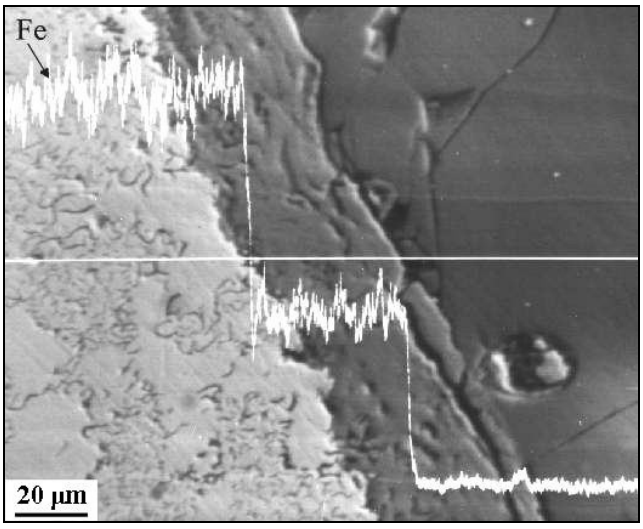

Fig. 8. An interface of slag clot and cast iron trickle No.2 (back-scattered electron image): cast iron trickle (light gray, with small graphite flakes) is separated from slag clot (dark) by iron oxide film (variously grey). Fe – iron concentration in corresponding phases

4. CONCLUSIONS

1. Carbon is a principal element defining the properties of cast iron. The other elements, silicon and phosphorus in particular, also affect the composition of the eutectic point in an alloy and, therefore, exert a certain influence on its properties. The carbon equivalent values (C.E.) of the Lieporian cast iron lump, taking into account the amount of Si and P, have been calculated following the recommendation [19]: C.E. = $C\%_{total}$ + 1/3(Si % + P %). The C.E. have been determined to be relatively high and ranging from 3.73 to 4.48. The liquidus temperature of cast iron having these C.E. values is pretty low, ca 1150 °C – 1220 °C. Hence, the melting point of the smelted cast iron could be of the same level as that of slag. However, high fluidity of fayalitic slag in the lump (formation of tin slag layers) suggests the ore smelting temperature could have reached about 1250 °C – 1300 °C.
2. White iron matrix of many of the trickles indicates rather considerable cooling rate in their solidification process. Probably, the lump was solidified in pretty cold environment, somewhere in the zone of a tap hole of furnace.
3. Morphology of the Lieporian lump and high heterogeneity of both chemical composition and microstructure suggests it as an accidental product formed during the bloomery smelting of iron ore containing some higher amount of manganese minerals, as compared with common ore.

Acknowledgements

The authors would like to thank archaeologist Mrs. Birutė Salatkienė and the authorities of Šiauliai museum "Aušra" for permission to sample this interesting finding. Special thanks are due to Professor Ingo Keesmann for making the arrangements for examination to be undertaken at Johannes Gutenberg University Mainz. The authors thank also Dr. Eimutis Matulionis (Institute of Chemistry, Vilnius) and Dr. Burkhard Schulz-Dobrick (Johannes Gutenberg University, Mainz) for their kind help in SEM analysis.

REFERENCES

1. **Straube, E.** Kritische Gegenüberstellung der Theorien über die Metallurgie des Rennfeuers *Ferrum* 57 1986: pp. 20 – 28.
2. **Roždzieński, W.** *Officina ferraria* or Smeltery and Workshop for Honourable Affair of Iron (Krakow 1612), Wrocław-Warszawa, 1964: pp. 164 – 176 (in Polish).
3. **Radwan, M**. Ores, Forges and Iron Blast-Furnaces in Poland. Warszawa, wyd. Naukovo-Techniczne, 1963: p. 61 (in Polish).
4. **Nosek, E.** Grapie is an Object for Investigation *Z otchłani wieków* XXX 1964: pp. 164 – 176 (in Polish).
5. **Hjärthner-Holdar, E., Kresten, P., Larsson, L.** Slags from Dala Airport, Dalecarlia, St.Tuna parish, RAÄ 382 *Activity Report* The Central Board of National Antiquities, UV Uppsala, 1997: pp. 13 – 15.
6. **Navasaitis, J., Pilkaitė, T., Sveikauskaitė, A., Matulionis, E.** Metallographic Analysis of the As-Smelted Bloomery Iron *Acta Metallurgica Slovaca* 7 2001: pp. 119 – 126.
7. **Senn Bischofberger, M.** Das Schmiedehandwerk im nordalpinen Raum von der Eisenzeit bis ins frühe Mittelalter *Internationale Archäologie: Naturwissenschaft und Technologie* 5 2005: p. 288.
8. **Fluzin, Ph.** Ponte di Val Gabbia III (Bienno). Les premiers résultats des études métallo-graphiques *Il ferro nelle Alpi – Iron in the Alps. Proceedings of the conference 1998 (C.Cucini Tizzoni, M.Tizzoni eds.)* Bienno, 2000: pp. 24 – 31.
9. **Kremer, M., Reif, W., Henkel, A.** Roemisches Roheisen in Dillingen/Saar *Stal und Eisen* 117 (8) 1997: pp. 150 – 151.
10. **Pleiner, R.** Cast Iron in the European Bloomery Period *Acta Metallurgica Slovaca* 7 2001: pp. 97 – 101.

11. **Knau, H. L., Beier, T., Sönnecken, M.** Iron Works and Water Power – the Development of Mechanical Hammer Works in the "Südgebirge" *Acta Metallurgica Slovaca* 7 2001: pp. 127 – 143.
12. **Salatkienė, B.** Research on the 1st Settlement in Lieporiai *Archeologiniai tyrinėjimai Lietuvoje 1996 ir 1997 metais* Vilnius, 1998: pp. 90 – 99 (in Lithuanian).
13. **Navasaitis, J.** Reconstruction of the Lieporian Bloomery Furnace *Kultūros paveldas* – 97. Vilnius, 1997: pp. 39 – 44 (in Lithuanian).
14. **Stankus, J.** Technology of Iron Artefacts from the Castle of Vilnius. *Early Iron Production – Archaeology, Technology and Experiments*, ed. By Lars Ch. Nørbach. Technical Report No. 3, Lejre, 1997: pp. 133 – 141.
15. **Navasaitis, J.** Lithuanian Iron. Kaunas, Technologija, 2003: pp. 22 ff (in Lithuanian).
16. **Swalin, R. A.** Thermodynamics of Solids. New York, John Wiley & sons, Inc., 1964: p. 72 ff.
17. **Efimenko, G. G., Gimmelfarb, A. A., Levchenko V. E.** Metallurgy of Cast Iron. Kiev, 1981: p. 226 ff. (in Russian).
18. **Tylecote, R. F.** Metallurgy in Archaeology. London, Edward Arnold Ltd, 1962: p. 192.
19. **Rollason, E. C.** Metallurgy for Engineers. London, Edward Arnold Ltd, 1965: p. 256.

DOI: 10.5755/j02.ms.26306